Optical measurement of the temporal delay between two ultra-short and focussed laser pluses

Corvan, D. J., Dzelzainis, T., Hyland, C., Nersisyan, G., Yeung, M., Zepf, M., & Sarri, G. (2016). Optical measurement of the temporal delay between two ultra-short and focussed laser pluses. *Optics Express*, *24*(3), 3127-3136. https://doi.org/10.1364/OE.24.003127

Published in:
Optics Express

Document Version:
Publisher's PDF, also known as Version of record

Queen's University Belfast - Research Portal:
Link to publication record in Queen's University Belfast Research Portal

Publisher rights
© 2016 The Authors
Published by The Optical Society under the terms of the Creative Commons Attribution 4.0 License, (https://creativecommons.org/licenses/by/4.0/), which permits unrestricted use, distribution and reproduction in any medium, provided the author and source are cited. Further distribution of this work must maintain attribution to the author(s) and the published article's title, journal citation, and DOI.

General rights
Copyright for the publications made accessible via the Queen's University Belfast Research Portal is retained by the author(s) and / or other copyright owners and it is a condition of accessing these publications that users recognise and abide by the legal requirements associated with these rights.

Take down policy
The Research Portal is Queen's institutional repository that provides access to Queen's research output. Every effort has been made to ensure that content in the Research Portal does not infringe any person's rights, or applicable UK laws. If you discover content in the Research Portal that you believe breaches copyright or violates any law, please contact openaccess@qub.ac.uk.

Download date:04. May. 2023

Optical measurement of the temporal delay between two ultra-short and focussed laser pluses

D. J. Corvan,[1,*] T. Dzelzainis,[1] C. Hyland,[1] G. Nersisyan,[1] M. Yeung,[1,2] M. Zepf,[1,2] and G. Sarri[1]

[1]*School of Mathematics and Physics, Queens University Belfast, BT7 1NN, Belfast, UK*
[2]*Helmoltz Institut Jena, Fröbelstieg 3,07743 Jena, Germany*
[*]*dcorvan01@qub.ac.uk*

Abstract: Temporal overlapping of ultra-short and focussed laser pulses is a particularly challenging task, as this timescale lies orders of magnitude below the typical range of fast electronic devices. Here we present an optical technique that allows for the measurement of the temporal delay between two focussed and ultra-short laser pulses. This method is virtually applicable to any focussing geometry and relative intensity of the two lasers. Experimental implementation of this technique provides excellent quantitative agreement with theoretical expectations. The proposed technique will prove highly beneficial for high-power multiple-beam laser experiments.

Published by The Optical Society under the terms of the Creative Commons Attribution 4.0 License. Further distribution of this work must maintain attribution to the author(s) and the published article's title, journal citation, and DOI.

OCIS codes: (120.0120) Instrumentation, measurement, and metrology; (140.0140) Lasers and laser optics.

References and links

1. A. Di Piazza, C. Müller, K.Z. Hatsagortsyan, and C. H. Keitel, "Extremely high-intensity laser interactions with fundamental quantum systems," Rev. Mod. Phys. **84** 1177 (2012).
2. A. Bruce, R. P. Drake and D. D. Ryutov, "Experimental astrophysics with high power lasers and *Z* pinches," Rev. Mod. Phys. **78** 755 (2006).
3. O. Lundh, J. Lim, C. Rechatin, L. Ammoura, A. Ben-Ismal, X. Davoine, G. Gallot, J-P. Goddet, E. Lefebvre, V. Malka, and J. Faure, "Few femtosecond, few kiloampere electron bunch produced by a laser plasma accelerator," Nat. Phys. **7** 219 (2011).
4. D. Umstadter, J. K. Kim, and E. Dodd, "Laser injection of ultrashort electron pulses into Wakefield plasma waves," Phys. Rev. Lett. **76** 2073 (1996).
5. A. R. Bell and J. G. Kirk, "Possibility of prolific pair production with high-power lasers," Phys. Rev. Lett. **101**, 200403 (2008).
6. C. Harvey, T. Heinzl, and A. Ilderton, "Signatures of high-intensity Compton scattering," Phys. Rev. A **79** 063407 (2009).
7. G. Sarri, D. J. Corvan, W. Schumaker, J. M. Cole, A. Di Piazza, H. Ahmed, C. Harvey, C.H. Keitel, K. Krushelnick, S. P. D. Mangles, Z. Najmudin, D. Symes, A. G. R. Thomas, M. Yeung, Z. Zhao and M. Zepf, "Ultrahigh brilliance multi-MeV γ-ray beams from nonlinear relativistic thomson scattering," Phys. Rev. Lett. **113** 224801 (2014).
8. K. Khrennikov, J. Wenz, A. Buck, J. Xu, M. Heigoldt, L. Veisz, and S. Karsch, "Tunable all-optical quasimonochromatic Thomson x-ray source in the nonlinear regime," Phys. Rev. Lett. **114** 195003 (2015).
9. S. Chen, N. D. Powers, I. Ghebregziabher, C. M. Maharjan, C. Liu, G. Golovin, S. Banerjee, J. Zhang, N. Cunningham, A. Moorti, S. Clarke, S. Pozzi, and D. P. Umstadter, "MeV-energy X rays from inverse Compton scattering with laser-Wakefield accelerated electrons," Phys. Rev. Lett. **110** 155003 (2013).
10. N. D. Powers, I. Ghebregziabher, G. Golovin, C. Liu, S. Chen, S. Banerjee, J. Zhang, and D. P. Umstadter, "Quasi-monoenergetic and tunable X-rays from a laser-driven Compton light source," Nat. Photonics **8** 28 (2014).

#253525 Received 10 Nov 2015; revised 2 Jan 2016; accepted 5 Jan 2016; published 5 Feb 2016
© 2016 OSA

11. F. Mackenroth and A. Di Piazza, "Nonlinear Compton scattering in ultrashort laser pulses," Phys. Rev. A **83** 032106 (2011).
12. J. Piasecki, B. Colombeau, M. Vampouille, C. Froehly, and J. A. Arnaud, "Nouvelle méthode de mesure de la réponse impulsionnelle des fibres optiques," Appl. Opt. **19** 3749 (1980).
13. D. Meshulach, D. Yelin, and Y. Silberberg, "Real-time spatialspectral interference measurements of ultrashort optical pulses," J. Opt. Soc. Am. B **14** 2095 (1997).
14. C. N. Danson, P. A. Brummitt, R. J. Clarke, J. L. Collier, B. Fell, A. J. Frackiewicz, S. Hancock, S. Hawkes, C. Hernandez-Gomez, P. Holligan, M. H. R. Hutchinson, A. Kidd, W. J. Lester, I. O. Musgrave, D. Neely, D. R. Neville, P. A. Norreys, D. A. Pepler, C. J. Reason, W. Shaikh, T. B. Winstone, R. W. W. Wyatt, and B. E. Wyborn, "Vulcan Petawatt an ultra high intensity interaction facility," Nucl. Fusion **44** S239 (2004).
15. Extreme Light Infrastructure, http://www.eli-beams.eu/
16. C.J. Hooker, J.L. Collier, O. Chekhlov, R. Clarke, E. Divall, K. Ertel, B. Fell, P. Foster, S. Hancock, A. Langley, D. Neely, J. Smith & B. Wyborn "The Astra Gemini project; A dual beam petawatt Ti:Sapphire laser system," J. Phys. IV France **133**, 673 (2006).

1. Introduction

The interaction of ultra-intense lasers with matter, can create extreme states whose study is of paramount importance for the understanding of high energy density physics. Multiple laser beam interactions are progressively attracting the attention of the physics community as they provide a unique scenario for the experimental study of highly non-linear particle-photon interactions [1], laboratory astrophysics [2], particle acceleration [3, 4], particle generation [5] and the production of the next generation of x-ray and γ-ray sources [6-11].

For a meaningful experimental implementation, it is indeed necessary that the high intensity foci of the lasers be spatially and temporally overlapped with a micron and femtosecond scale precision respectively. While spatial overlap is relatively easy to achieve, femtosecond scale temporal overlap is a much harder task, since it lies orders of magnitude below the typical resolution of electronic devices (which respond on the ns to 100's of ps scale).

Previously, it was shown that by using the relatively broad frequency envelope of a femtosecond laser pulse, detailed information about the phase front and relative time delay between two collimated laser pulses could be revealed by employing an interferometric technique provided prior knowledge of a reference beam parameters was obtained [12, 13]. Exploiting similar physical principles, we report here on a compact and versatile experimental technique that allows for the precise measurement of the temporal delay between two short laser pulses at their focal planes while simultaneously allowing for micron scale overlapping in the plane perpendicular to the axis of propagation of the pulses. The proposed technique can be implemented in virtually any focusing geometry and relative intensity of the two pulses and has been tested with the oscillator of the TARANIS femtolab at Queen's University Belfast (QUB) which has an energy of 6.6 nJ and a pulse duration of $T_0 = 140$ fs. The repetition rate of the system is 76 MHz with a wavelength of 800 with 32 nm FWHM.

This technique will prove highly beneficial for the next class of multi-petawatt laser systems such as the 20 PW Vulcan at Rutherford Appleton Laboratories (RAL) [14] and the Extreme Light Infrastructure (ELI) [15], in which experiments with multiple ultra-high intensity lasers will be routinely performed.

The structure of this paper is as follows. In Section 2 the theory underlying this technique will be discussed and a prediction of the outcome is provided based on data specific to TARANIS. Then in Section 3, the implementation of the technique is outlined for this facility. Section 4 presents the experimental findings and a comparison with the predictions is made. Finally, Section 5 gives a conclusive overview of the technique.

#253525 Received 10 Nov 2015; revised 2 Jan 2016; accepted 5 Jan 2016; published 5 Feb 2016
© 2016 OSA

2. Theoretical Rationale

The electric field of an electromagnetic wave can be expressed generally as $E = E_0 e^{-i(k\cdot r-\omega\tau-\phi_0)}$ where E_0 is the peak electric field strength, k is wavevector ($2\pi/\lambda$ where λ is the wavelength of the pulse), r is the displacement vector from the source to the point of observation, ω is the frequency of the wave, τ is the time of observation of the pulse and ϕ_0 is a constant. The general equation describing the intensity of electromagnetic radiation is given by $I = c\varepsilon_0 |EE^*|/2$ where c is the speed of light and ε_0 is the permittivity of free space.

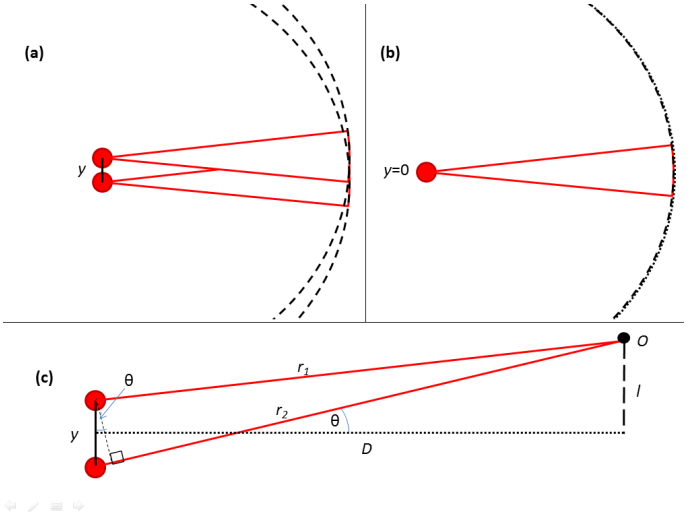

Fig. 1. (a) The sources of two spherical wavefronts are separated in space by a transverse distance y, an angular difference can be seen by an observer at O. As shown in (c), the observer is at a distance D and height l above the common centre of the sources giving an angle of θ. For this case the paths r_1 and r_2 are slightly different and the wavefronts will form an interference pattern. (b) when $y \to 0$ the angle between the two pulses as seen by an observer at O tends to 0. In this case, no such pattern is observed. In the case where $y \ll D$ the spatial relationship can be written as $r_2 = r_1 + y\sin\theta$

From Fig. 1, it can be seen that the superposition of two electromagnetic waves with a similar peak field strength E_0, gives an intensity

$$I = c\varepsilon_0 E_0^2 \left|1 + \cos\left[(k_1 \cdot r_1 - k_2 \cdot r_2 - \omega_1\tau_1 + \omega_2\tau_2 + \phi_1 - \phi_2)\right]\right| \tag{1}$$

If we consider the first wave to be propagating along r_1 and the second wave to be propagating at an angle θ separated by y with respect to this so that $r_2 = r_1 + y\sin\theta$ (where y is the distance separating the two sources of the waves), and the waves to have identical frequencies, with a temporal delay related by $\tau_2 = \tau_1 + \Delta\tau$, then the Eq. (1) becomes

$$I \propto \left|1 + \cos[ky\sin\theta - \omega\Delta\tau + \phi]\right| \tag{2}$$

In Eq. (2) the notation 1 has been dropped for convenience, in addition the constants have been replaced by $\phi = \phi_1 - \phi_2$. This equation can be thought of as consisting of two distinct parts, a spatial component which varies periodically with θ and a temporal component which varies periodically with $\Delta\tau$ demonstrating that Eq. (2) varies periodically.

If we consider two realistic laser pulses of identical bandwidth $\Delta\lambda$ and central wavelength λ_0, the use of a diffraction grating allows two pulses to interfere spectrally many pulse durations

#253525 Received 10 Nov 2015; revised 2 Jan 2016; accepted 5 Jan 2016; published 5 Feb 2016
© 2016 OSA

apart. If the diffraction grating disperses the various spectral components in one axis only, then this behaviour will only manifest in the dispersion axis [12]; let this phase term be $\vartheta = \omega\Delta\tau$.

In order to improve the resolution of the system, a lens can be used after the grating. The focussing power of the lens will smooth modulations induced by the spatial interference along the axis of dispersion. A cylindrical lens allows one to remove this information in one axis while allowing it to persist in the other. Hence, the phase term representing spectral information ϑ, appears exclusively along the dispersion axis.

In the undispersed, unfocused (with respect to the cylindrical lens) axis, perpendicular to the axis in which spectral components manifest, the spatial contributions are present while spectral components are not. Considering the simple 2-point source diffraction equation from Young's Double slit experiments (see Fig. 1) the spatial terms can be written as $\varphi = ky\sin\theta$.

In order to determine the intensity for an observer at any point, the solution will be proportional to the cosine of the sum of the temporal domain ϑ and spatial domain φ as shown below.

$$I(\vartheta,\varphi) \propto \left|1+\cos(\vartheta+\varphi)\right| \tag{3}$$

Eq. (3) allows one to make a prediction of the interference pattern that would be observed if a CCD were placed in the arrangement.

3. Experimental Setup

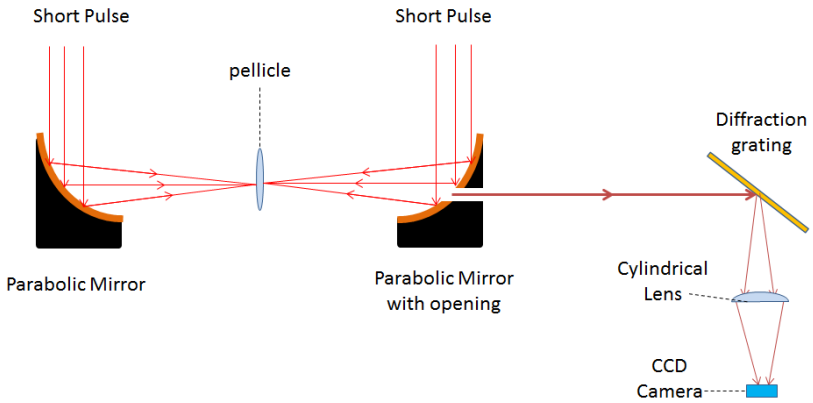

Fig. 2. Two counter-propagating laser pulses are incident on the pellicle whose surface closest to the parabolic mirror with the hole represents the point at which temporal delay is measured. The focal spot of the parabolic mirror with the hole in it is directly on the surface of the pellicle. The pellicle is then angled very slightly to allow the reflection off the surface to propagate through the opening in the parabola. The second pulse is transmitted on axis through the pellicle and through the opening of the next parabola. The sampled component of the pulses is incident on a diffraction grating. A cylindrical lens is used to increase the resolution of the system and destroy the spatial components along the spectrally dispersed axis. The CCD reads out the intensity pattern arising from the pulses.

In most modern laser facilities, the intensity of laser pulses is greatly increased by focusing via parabolic mirrors. The rise of dual-pulse, counter-propagating geometries such as that shown in reference [7], may require the employment of such mirrors which have been modified with a hole in their centre in order to allow electrons generated by laser wakefield acceleration to propagate unhindered by the physical presence of the mirror.

#253525 Received 10 Nov 2015; revised 2 Jan 2016; accepted 5 Jan 2016; published 5 Feb 2016
© 2016 OSA

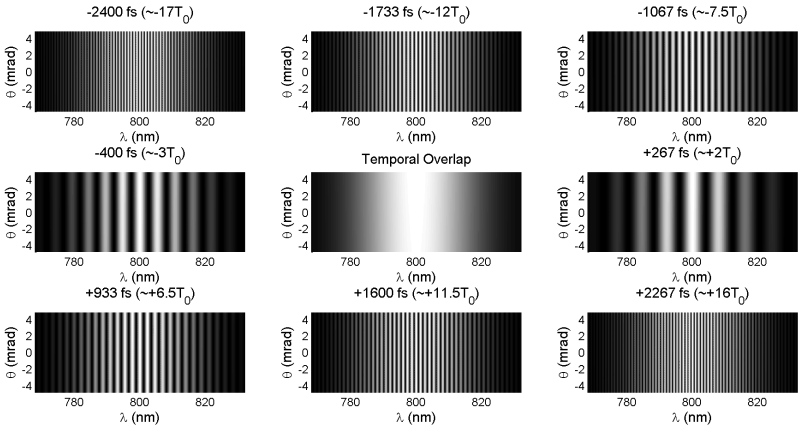

Fig. 3. With the vertical axis representing the relative angle the observer is at from the common centre of the origin of the two pulses θ and the and the horizontal axis representing the wavelengths λ, present, the relative intensity is plotted. Values are determined by adding summing the spectral and temporal phase differences and substituting into Eq. (3). With perfectly overlapped focal planes, spatial differences should be negligible and the temporal terms are the main contributors to the pattern. Moving through the diagrams, the relative temporal delay between the pulses is given above each pattern. Fringes are vertical and are observed to become wider as the time difference between the pulses decreases to 0. The central image represents the pattern at best temporal match. The 9 images begin from the top left at a time delay of $-2400(\sim -17T_0)$, $-1733(\sim -12T_0)$, $-1067(\sim -7.5T_0)$, $-400(\sim -3T_0)$ fs before temporal overlap is reached. The process then proceeds to times of $+267(=\sim 2T_0)$, $+933(\sim 6.5T_0)$, $+1600(\sim 11.5T_0)$ and $+2267(\sim 16T_0)$ fs.

Hence, the technique outlined in Section 2 was investigated for a counter-propagating arrangement where two pulses are required to arrive simultaneously at a point; this is marked by the placement of a thin pellicle (see Fig. 2).

In this arrangement, a 50.8 mm parabolic mirror of focal length 101.1 mm with a 3 mm hole in the substrate, and 8 mm at the point of exit at the back of the mounting, is focused onto surface of the pellicle. The pellicle is angled very slightly to allow the reflection off the surface to propagate through the opening in the parabola. The second pulse is focussed by a second parabola of the same parameters (however, without the hole) and is transmitted on axis through the pellicle. The transmitted and reflected components of the pulses which propagate through the hole in the parabola and are incident on a diffraction grating of 800 lines per mm which is placed 530 mm from the back of the holed parabola and angled such that the first order reflection of diffraction from it is 50 mm from a cylindrical lens of focal length 50 mm. A CCD is placed 60 mm after the lens.

To improve the fringe contrast seen by the CCD, one may require a method to control the relative intensities without inducing any path difference in one pulse with respect to the other, for this identical polarisers can be placed into the arrangement, one before each parabolic mirror if the beams are polarised in the same plane (where one can be screened out with respect to the other), or one directly after the hole for the case of cross polarised pulses (to allow simultaneous control of relative intensities and allow the two pulses to gain common axial components). The sampled components of the pulses are incident on a diffraction grating then propagate through a cylindrical lens. This destroys any spatial information gained in the arrangement

#253525 Received 10 Nov 2015; revised 2 Jan 2016; accepted 5 Jan 2016; published 5 Feb 2016
© 2016 OSA

while simultaneously allowing the resolution of the components to be improved. The CCD reads out the intensity pattern arising from the pulses. This is shown in Fig. 2.

Using the specifications of the TARANIS oscillator outlined in the first section expectations of an intensity pattern of two overlapping pulses can be determined. Initially the focal spots of the two pulses are overlapped using a thin wire and CCD camera as is standard in most laser facilities. If the pulses are overlapped perfectly, y and θ both drop to 0. This means that there are no spatial terms in Eq. (3); a prediction is shown in Fig. 3.

As can be seen in Fig. 3, when the time delay is increased, the fringe separation decreases also. Moving through the diagrams, fringes are vertical and are observed to become wider as the time difference reduces to 0. The central image represents the pattern at temporal overlap stretches across the full bandwidth. Far from temporal overlap, the fringes tend towards being infinity close and are unable to be resolved, in this setup, this occurred at $\sim 20T_0$.

Figure 3 represents the case where the foci of the pulses are perfectly overlapped; in the case where the offset is set to 250 μm, one can see the change that occurs to the pattern governed by Eq. (3) is entirely due to $\vartheta \neq 0$. This results in a fixed firing pattern being present in the θ axis. As the φ remains unaffected, the pattern becomes modified such that the fringes are now angled (this angle will be specific to the distance of the CCD from the pellicle). Assuming a CCD at a distance of 1.0 m from the pellicle, a fringe pattern is given in Fig. 4.

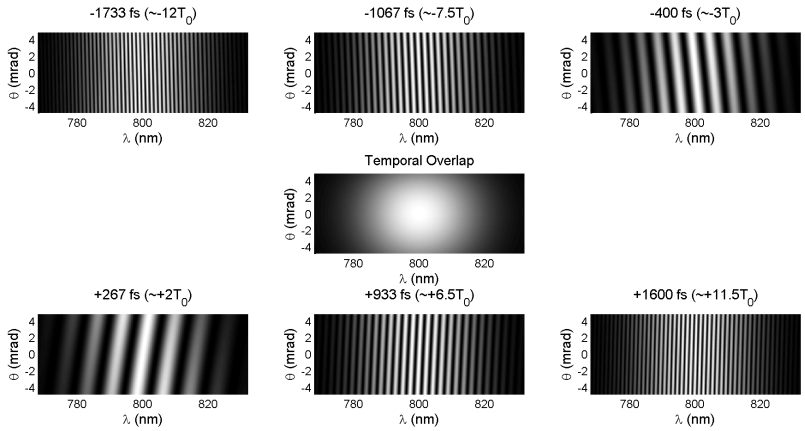

Fig. 4. With the vertical axis representing the relative angle the observer is at from the common centre of the origin of the two pulses θ and the and the horizontal axis representing the wavelengths λ, present, the relative intensity is plotted. Values are determined by adding summing the spectral and temporal phase differences and substituting into Eq. (3). With the pulses now separated by 250 μm the spatial term makes a contribution. The result is a fringe pattern that is slanted. The behaviour of the temporal fringes remain unaffected. The 7 images begin from the top left at a time delay of $-1733(\sim -12T_0)$, $-1067(\sim -7.5T_0)$, $-400(\sim -3T_0)$ fs before temporal overlap is reached. The process then proceeds to times of $+267(\sim 2T_0)$, $+933(\sim 6.5T_0)$ and $+1600(\sim 11.5T_0)$ fs.

As demonstrated in Figs. 3 and 4, for each time delay given, a unique number of fringes is present along the λ axis. The number of these temporal fringes which are present is of course related to the bandwidth of the system being used; however, as a consequence of this, simply counting the number of temporal fringes present the user is able to obtain information regarding the relative temporal mis-match of the pulses.

#253525 Received 10 Nov 2015; revised 2 Jan 2016; accepted 5 Jan 2016; published 5 Feb 2016
© 2016 OSA

4. Results

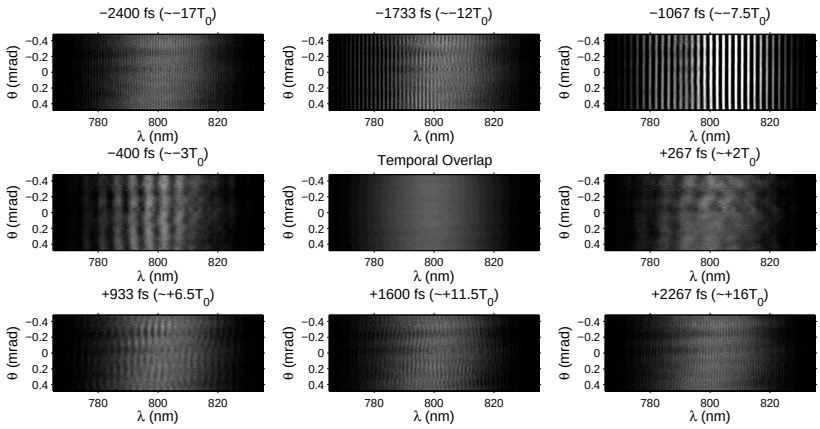

Fig. 5. Results of the temporal matching process as seen on the CCD camera. The 9 images begin from the top left at a time delay of $-2400(\sim -17T_0)$, $-1733(\sim -12T_0)$, $-1067(\sim -7.5T_0)$, $-400(\sim -3T_0)$ fs before best temporal overlap is reached. The process then proceeds to times of $+267(\sim 2T_0)$, $+933(\sim 6.5T_0)$, $+1600(\sim 11.5T_0)$ and $+2267(\sim 16T_0)$ fs. It can be seen that the fringes are vertical in orientation and begin compressed. The reduction of the temporal delay leads to the broadening of the fringes until temporal overlap where the the broadening tends to a single fringe which stretches over the full bandwidth. After this point, increasing the temporal delay leads to a compression of the fringes, mirroring the behaviour of the fringes prior to temporal overlap.

Using the setup presented in the previous section, results were obtained in order to make a comparison with the theoretical expectations. Looking at Fig. 5, one can see the changes that occur on the CCD camera close to temporal overlap. The 9 images begin from the top left at a time delay of $-2400(\sim -17T_0)$, $-1733(\sim -12T_0)$, $-1067(\sim -7.5T_0)$, $-400(\sim -3T_0)$ fs before temporal matching occurs. The process then proceeds to times of $+267(\sim 2T_0)$, $+933(\sim 6.5T_0)$, $+1600(\sim 11.5T_0)$ and $+2267(\sim 16T_0)$ fs. The central image shows the pattern obtained at temporal overlap.

Progressing from the upper left to the central image in Fig. 5, one can see the fringes begin to expand until temporal overlap; at this point, no fringes can be seen. This is within the expectations discussed previously in Section 2. Continuing through the images from the central image to lower right of the figure, the behaviour of the fringes is mirrored and the fringes begin to once again, compress.

Using Figs. 3 and 5, a comparison between the number of temporal fringes expected theoretically and those obtained experimentally along the λ axis was made. Figure 6 shows that a similar number of fringes are present in the experimental findings to the number predicted in the theoretical model presented in Fig. 3. The number of fringes determined experimentally are generally lower than those predicted; however, this is most likely due to the poor contrast of the fringes in the peripheral regions of the images. The gradient of the graph presented in Fig. 6 is shown to be $\Delta\omega$ i.e., the range of frequencies contained within the pulse packet. In terms of the bandwidth of the laser, this is approximately

$$\frac{N}{\Delta\tau} \approx \left| \frac{c\Delta\lambda}{\lambda_L^2} \right| \tag{4}$$

#253525 Received 10 Nov 2015; revised 2 Jan 2016; accepted 5 Jan 2016; published 5 Feb 2016
© 2016 OSA

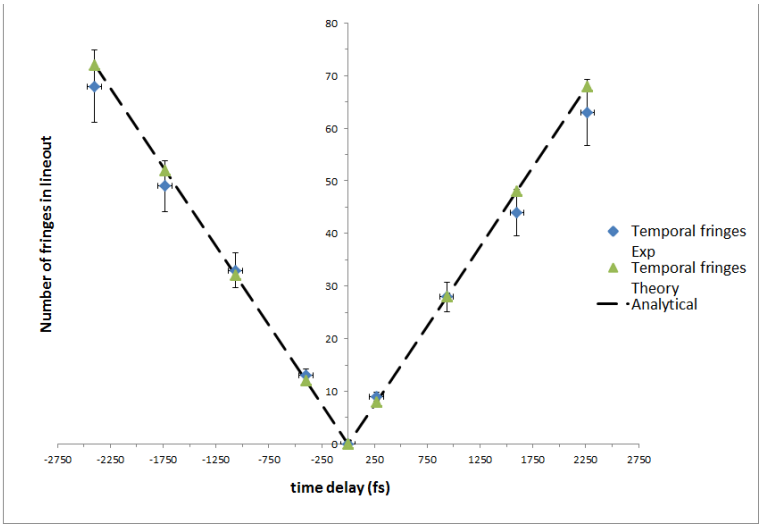

Fig. 6. A comparison between the theoretical expectations of the number of temporal fringes predicted (green) in the model presented in Fig. 3 and the number of fringes detected in the experimental setup (blue). The trend is the modulus of a linear relationship. In this case, the uncertainty in the time is a result of the maximum precision of the delay stage. This can be improved by use of more precise equipment. As the technique allows for temporal matching of the pulses without prior calibration of the spectrometer , the uncertainty presented in the number of fringes recorded is a result of the poor contrast of the fringes in the peripheral regions of the images. The line represents the gradient of $c|\Delta\lambda/\lambda_L^2|$

Where N is the number of fringes that are observed on the CCD. This result demonstrates that a user is able to establish with the most basic information about a laser system, the time delay between two pulses. By varying the number of fringes on the CCD, one can determine the delay between two intense laser pulses. In Fig. 6 the uncertainty in the number of fringes detected can be attributed to the poor contrast seen at the edges of the intensity pattern on the CCD and estimated at $\sim 10\%$. By carrying out a Fourier analysis on the fringe pattern, in order to extract the separation, the results are extremely similar; however, this technique improves the accuracy to $< 1\%$. It is important point to note that one of the strengths of the technique lies in requiring no prior calibration which can save valuable time in an experimental environment. Clearly, the degree of temporal matching is limited by the accuracy of the delay stage, in this instance be achieved within ± 66 fs. This is easily improved by the use of more precise equipment. And while improving the arrangement by use of different lenses and/or gratings, Eq. (4) can be used to determine an absolute limit to the precision of the technique by rearranging the equation so we have

$$\Delta\tau = \frac{N\lambda_L^2}{c\Delta\lambda} \tag{5}$$

In this particular system, this was found to be ± 33 fs i.e., the time difference between the two pulses that will add another fringe to the pattern. For a broader bandwidth, this of course will improve.

In the case where the temporal matching process is carried out with a misalignment of the focal spots of 250 μm, the 7 images begin from the top left at a time delay of $-1733(\sim -12T_0)$, $-1067(\sim -7.5T_0)$, $-400(\sim -3T_0)$ fs before temporal matching is reached. The process then proceeds to times of $+267(\sim 2T_0)$, $+933(\sim 6.5T_0)$ and $+1600(\sim 11.5T_0)$ fs. It can be seen

#253525 Received 10 Nov 2015; revised 2 Jan 2016; accepted 5 Jan 2016; published 5 Feb 2016
© 2016 OSA

that the fringes no longer simply vertical in orientation. This is due to a spatial difference being present on the vertical axis. The fringes do begin compressed and expand as the temporal overlap is approached, this time however, they also rotate. This is shown in Fig. 7. The rotation is of course dependant on the arrangement of the setup, particularly the distances to and size of CCD chip as well as power and distance of the lens. The process has also been tried for

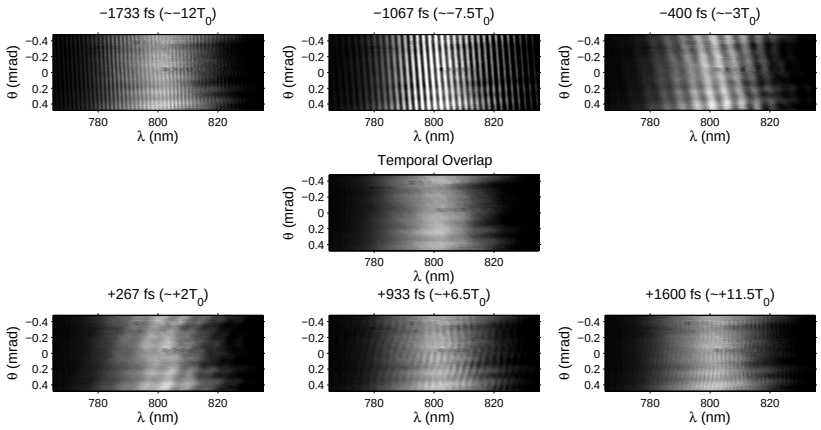

Fig. 7. Results of the temporal matching process as seen on the CCD camera when a misalignment of the focal spots at 250 μm is introduced. The 7 images begin from the top left at a time delay of $-1733(\sim -12T_0)$, $-1067(-\sim 7.5T_0)$, $-400(-\sim 3T_0)$ fs before temporal overlap is reached. The process then proceeds to times of $+267(\sim 2T_0)$, $+933(\sim 6.5T_0)$ and $+1600(\sim 11.5T_0)$ fs. It can be seen that the fringes no longer simply vertical in orientation. This is due to a spatial difference being present on the vertical axis. The fringes do begin compressed and expand as temporal overlap is approached, this time however, they also rotate.

two focal planes which have been separated by a few cm along the beam propagation axis. As expected, no difference is observed in the pattern of the CCD. This means that the process can be applied to virtually any short pulse setup which requires fs scale temporal matching.

As a final statement, the technique was repeated for focal spots at several centimetres apart, with the parabola marking the point at which the pulses are to be temporally overlapped. These results where very close to those presented for the overlap scenario presented above and will not be shown here; however, it is important to note the versatility of the technique as applied to different focussing geometries.

5. Conclusions

A method for real-time optical measurement of the temporal delay between two focussed and ultra-short laser pulses is presented. By varying the number of fringes on the CCD, one is able to determine with the delay between two intense laser pulses. In this case, we have achieved this to with an uncertainty of ± 66 fs i.e., the precision of the delay stage used. It has been shown that the degree of temporal overlap achievable, limited by a number of factors such as the step size available on the delay stage used, the resolution of fringes on the CCD and the number of lines per mm on the diffraction grating. However, assuming the impact of these factors can be minimised, a theoretical limit to the accuracy of the technique has been presented in Eq. (5).

Due to the compact and versatile nature of the technique, it should prove highly beneficial in reducing the technical difficulties that may arise specifically in the next class of multi-petawatt

#253525 Received 10 Nov 2015; revised 2 Jan 2016; accepted 5 Jan 2016; published 5 Feb 2016
© 2016 OSA

laser systems such as the 20 PW Vulcan at the Rutherford Appleton Laboratory and the Extreme Light Infrastructure, in which experiments with multiple ultra-high intensity lasers will be routinely performed. This technique has already been employed in a recent experimental campaign [7] carried out at the Astra Gemini facility at RAL [16] were the precision achievable was increased to ± 15 fs demonstrating its viability as a beneficial technique in the modern laser laboratory.

Acknowledgements

G. Sarri wish to acknowledge the financial support from EPSRC (grant number EP/L013975/1).

#253525 Received 10 Nov 2015; revised 2 Jan 2016; accepted 5 Jan 2016; published 5 Feb 2016
© 2016 OSA